International Journal of Advance Research in Science and Engineering
Volume No 06, Special Issue No. 03, September 2017, AFM-2017
www.ijarse.com
IJARSE
ISSN: 2319-8354

Synthesis and Spectral Studies of Co(II), Ni(II), Cu(II), Zn(II) and VO(IV) Complexes of a N, N, O-Donor N^4-phenyl semicarbazone: Antimicrobial, Antioxidant and DNA Cleavage Activities of the Semicarbazone and its Copper Complex

S. R. Layana[1], S. R. Saritha[2], L. Anitha[3], M. R. Sudarsanakumar[4]

[1,2,3,4,] *Department of Chemistry, Mahatma Gandhi College, University of Kerala, Thiruvananthapuram, Kerala, (India)*

ABSTRACT

We have synthesized Co(II), Ni(II), Cu(II), Zn(II) and VO(IV) complexes of N,N,O donor pyridine-2-carboxaldehyde–N^4–phenylsemicarbazone (HL). They were physicochemically characterized by elemental analysis, magnetic susceptibility and conductivity measurements, FT–IR, UV–Visible, mass and EPR spectral methods. The semicarbazone coordinates through keto or enol form in the complexes. The mass spectra of the complexes explain the metal-ligand ratio and hence their structure. The semicarbazone and its copper(II) complex were screened for antimicrobial, antioxidant and DNA cleavage activities.

Keywords-- pyridine-2-carboxaldehyde–N^4–phenylsemicarbazone, Mass spectrometry, antimicrobial activity, DPPH assay, DNA cleavage activity.

1. INTRODUCTION

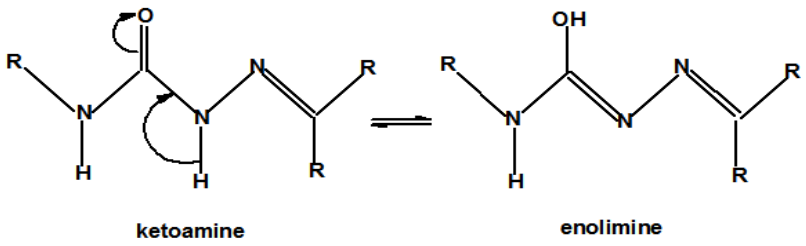

Scheme 1 ketoamine–enolimine tautomerism

Semicarbazones remain the central area of research during the past few decades due to their adaptable structural features. They are condenzation products of a semicarbazide and a suitable aldehyde or a ketone. Their tendency to exist either as neutral ketoamine or as deprotonated monoanionic enolimine

tautomeric form (Scheme 1) has made them versatile ligands in coordination chemistry [1]. Their ligational behaviour may vary with aldehydes or ketones having additional donor atoms [2].

Their coordinating ability is related to the extended delocalization through them, which will further boosted by the presence of hetero atoms and substitution at N^4 position. They show a wide variety of pharmacological applications including antibacterial, antifungal, anti HIV, anticancer, antineoplasic, hypolipidemic and anticonvulsant [3-6]. The biological properties of semicarbazones are related to metal ion coordination, which enhance their ability to pass through cell membranes. Apart from their biological relevances, they are also associated with analytical applications. In organic synthesis, semicarbazones are adopted as protective groups for carbonyl compounds [7-8].

Literature reviews reported the studies regarding the synthesis of HL and its complexes and their biological importances [9-11]. The synthesis and crystal structure of pyridine-2-carboxaldehyde-N(4)-phenyl semicarbazone is reported earlier [12]. The present study describes the synthesis and characterization of Co(II), Ni(II), Cu(II), Zn(II) and VO(II) complexes of N(4)-phenyl semicarbazone of pyridine-2-carboxaldehyde and the antimicrobial, antioxidant and DNA cleavage investigations of HL and its copper complex.

2. EXPERIMENTAL

2.1 Materials

AR grade Pyridine-2-carboxaldehyde (Alfa–Aesar) and N–(4)–phenyl semicarbazide (Alfa–Aesar), metal salts, $Co(NO_3)_2{\cdot}6H_2O$, $Ni(NO_3)_2{\cdot}6H_2O$, $Cu(NO_3)_2{\cdot}3H_2O$, $Zn(SO_4)_2{\cdot}7H_2O$ and $VO(SO_4){\cdot}XH_2O$ (All are Merck AR grade) and the solvents (methanol and ether) were used as purchased.

2.2 Synthesis of pyridine-2-carboxaldehyde-N^4–phenylsemicarbazone (HL)

Hot methanolic solutions of pyridine-2–carboxaldehyde (10 mmol) and N(4)–phenylsemicarbazide (1.511 g, 10 mmol) were mixed and refluxed for 5 hour after adjusting the P^H to 4.5. On slow evaporation, colourless crystals separated out (Scheme 2). They were filtered, washed with methanol and dried over P_4O_{10} in vacou. Single crystals of the title compound suitable for X–ray analysis were obtained by slow evaporation of solution in methanol for few days.

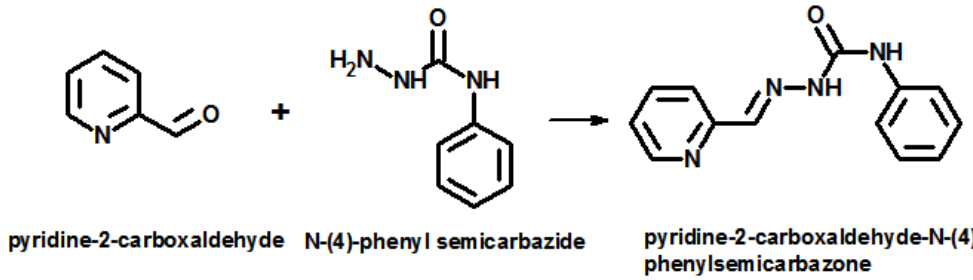

Scheme 2 Synthesis of pyridine–2–carboxaldehyde–N^4–phenylsemicarbazone

2.3 Synthesis of complexes

2.3.1 Synthesis of $[Co(L)(NO_3)]\cdot 2H_2O$ **(1)**

The complex was synthesized by refluxing hot methanolic solutions of HL (0.240 g, 2 mmol) and cobalt (II) nitrate hexahydrate (0.146 g, 1 mmol) for 3h. The dark brown solid formed was filtered, washed with hot methanol followed by water and ether and dried. It was recrystallized from methanol solvent. Yield: 70 %.

2.3.2 Synthesis of $[Ni(L)(NO_3)]$ **(2)**

Hot methanolic solutions of HL (0.240 g, 2 mmol) and nickel (II) nitrate hexahydrate (0.145 g, 1 mmol) were mixed and refluxed for 4h. The dark green solid formed was collected, washed, dried and recrystallized from methanol. Yield: 74 %.

2.3.3 Synthesis of $[Cu(L)_2]$ **(3)**

Equimolar amounts of HL (0.240 g, 2 mmol) and copper (II) nitrate trihydrate (0.240 g, 2 mmol) in hot methanol solution was reluxed for about 2h. The green colour precipitate formed were collected, washed with hot methanol, ether and water and recrystallized from methanol. Yield: 75%.

2.3.4 Synthesis of $[Zn(HL)(SO_4)(OMe)]\cdot H_2O$ **(4)**

The zinc complex was synthesized by mixing a hot methanolic solution of HL (0.240 g, 1 mmol) with zinc (II) sulfate heptahydrate (0.287 g, 1 mmol) in distilled water. The reaction mixture was then refluxed for 3h. The light yellow precipitate formed was filtered, washed thoroughly with water, hot methanol and ether and dried. Yield: 74 %.

2.3.5 Synthesis of $[(VO)(L)(OMe)]$ **(5)**

Refluxing hot methanolic solution of HL (0.240 g, 1 mmol) was mixed with a solution of vanadyl (II) sulfate (0.163 g, 1 mmol) in hot distilled water for 4h. The greenish yellow precipitate formed was filtered, washed and dried. Yield: 76 %.

2.4 Physical Measurements

The elemental analyses of the ligand and the complexes were carried out using Vario EL–III CHNS analyzer. The electronic spectra of the compounds were recorded using Varian Cary 5000 spectrometer in the range 200–1200 nm. The IR spectra were recorded on a Thermo Nicolet Avatar 370 DTGS spectrometer using KBr pellets in the range 4000–400 cm^{-1}. The NMR spectra (both ^{1}H NMR and ^{13}C NMR) of the ligand and the zinc (II) complex in DMSO solvent were recorded on Bruker Avance III**,** 400 MHz FT NMR spectrometer at SAIF, CUSAT, Kochi. The mass spectra were recorded in HREMI, Thermo Scientific Exactive System at NIIST, Thiruvananthapuram. The molar conductivities of the complexes were measured in 10^{-3} M DMF solutions using a Systronic model 303 direct reading conductivity meter. Room temperature magnetic susceptibility measurements were carried out using a Lakeshore 7410 model Vibrating Sample Magnetometer (VSM), at Indian Institute of Technology, Chennai, India.

2.5 Biological Studies

2.5.1 Antimicrobial screening

The antimicrobials present in the samples were allowed to diffuse out into the medium and interact in a plate freshly seeded with the test organisms. The resulting uniformly circular zones of inhibition were measured by measuring the diameter of zone of inhibition in centimeters. The antibacterial activity was evaluated using Muller Hinton Agar plates, while the antifungal activity was assessed by Potato Dextrose agar plates.

2.5.2 Antioxidant Assay

The antioxidant activity or radical scavenging activity of the compounds was determined by using DPPH (1,1-diphenyl-2-picryl hydrazyl) assay [13]. Different volumes (1.25 µl – 20 µl) of samples were made up to a final volume of 20 µl with DMSO and 1.48 ml DPPH (0.1 mM) solution was added. The reaction mixture incubated in dark condition at room temperature for 20 minutes. After 20 minutes, the absorbance of the mixture was read at 517 nm. 3 ml of DPPH was taken as control. Antioxidants react with DPPH and reduce it to DPPH-H and as consequence the absorbance decreases. The degree of discoloration indicates the scavenging potential of the antioxidant compounds or extracts in terms of hydrogen donating ability.

$$\% \text{ inhibition} = \frac{control - test}{control} X100$$

2.5.3 *In vitro* DNA cleavage Assay

DNA cleavage assay was performed using pUC 18 plasmid DNA (Harbone et al, 1998) through Agarose gel electrophoresis. A tube with plasmid was kept as negative control and one with 10µl of Fenton's reagent (30mM H_2O_2, 50mM ascorbic acid and 50mM $FeCl_3$) as positive control. The DNA fragments were separated by charge and size and move through agarose gel matrix, when subjected to an electric field across an electrolyte solution (buffer). When boiled in an aqueous buffer, agar dissolve and upon cooling solidifies to a gel. 1.5% agarose gel was prepared in 1x TE buffer and melted in hot water bath at 90˚C.Then the melted agarose was cooled down to 45˚C. 6µl of 10 mg/ml of ethidium bromide was added and poured in to gel casting apparatus with the gel comb. After setting, the comb was removed from the gel. The electrophoresis buffer was poured in the gel tank and the platform with the gel was placed in it so as to immerse the gel. The gel was loaded with the samples and run at 50 V for 30 minutes. The stained gel was visualized using a gel documentation system (E gel imager, Invitrogen).

3 RESULTS AND DISCUSSION

3.1 Analytical measurements

The conductivity and magnetic susceptibility values and the C, H, N data of the compounds are given in Table 1. The measured values of room temperature conductivity measurements for all the complexes fall in the range 7–21 $ohm^{-1}cm^2mol^{-1}$, indicating the non-electrolyte behaviour of the complexes [14]. All the complexes are associated with magnetic moment value corresponding to the number of unpaired electrons present in them. The cobalt complex has a magnetic moment of 4.67, which is close to that expected for a d^7 tetrahedral geometry [15]. This high value eliminates the possibility of a square planar geometry. The nickel complex shows a μ_{eff} value of 3.41 BM, due to two unpaired electrons in highspin system. This larger value gives evidence for the occurrence of a tetrahedral d^8 highspin system [16]. The μ_{eff} value for the copper complex is 1.72 BM, indicating monomeric d^9 highspin system [17]. The oxovanadium complex gives an effective magnetic moment of 1.66, near to that reported for a d^1 system.

Table 1

Analytical data of HL and complexes

Compound	Found (Calc) %			μ (BM)	Λ_M*
	C	H	N		
HL	65.45 (65.00)	5.07 (5.00)	23.68 (23.33)	——	——
$[Co(L)(NO_3)]\cdot 2H_2O$ (**1**)	39.72 (39.40)	4.01 (3.78)	17.47 (17.67)	4.67	16
$[Ni(L)(NO_3)]$ (**2**)	43.63 (43.37)	3.36 (3.05)	19.14 (19.46)	3.41	7
$[Cu(L)_2]$ (**3**)	57.42 (57.67)	4.28 (4.06)	20.37 (20.68)	1.72	21
$[Zn(HL)(SO_4)(OMe)]\cdot H_2O$ (**4**)	37.61 (37.30)	3.58 (3.77)	12.49 (12.43)	Diamagnetic	10
[(VO)(L)(OMe)] (**5**)	46.02 (46.29)	4.25 (4.15)	16.48 (16.62)	1.66	13

***Molar conductivity (Ω^{-1} cm^2 mol^{-1}) taken in 10^{-3} M DMF solution**

3.2 IR Spectra

The IR spectra are displayed in Figs. 1 to 6. The spectral assignments are summarized in Table 2. The peak due to azomethine bond of HL is downshifted in all the complexes in the range 1545-1568 cm^{-1}, evincing the azomethine coordination during complex formation [18]. Presence of a new band in the complexes near 417-512 cm^{-1} region, owing to M–N stretching also supports the azomethine

coordination [19]. The upshifted N–N stretching frequency in complexes again affirms the C=N coordination. This positive shift is attributted to the increase in the double bond character, to counterbalance the loss of electron density through donation to the metal. The disappearance of C=O stretching frequency and the ^{2}N-H frequency of the ligand at 1694 cm^{-1} and 3376 cm^{-1} during complexation gave a clear evidence for enolic coordination of HL in theses complexes excluding **4**. Moreover, in these complexes there is a sharp peak in the range 1489-1540 cm^{-1} due to the newly formed N=C bond after enolization. The M–O band in the range 505–612 cm^{-1} in the complexes also suggests the keto or enol coordination [19]. The strong peak at 613 cm^{-1} in the free ligand due to pyridine ring vibration, is shifted positively in all complexes (679-696 cm^{-1}), indicating pyridine nitrogen coordination during metal coordination [10].

There are absorptions at 1384 cm^{-1}, 1290 cm^{-1} and 1210 cm^{-1} for **1** and at 1324 cm^{-1}, 1230 cm^{-1} and 1050 cm^{-1} for **2** due to monocoordinated nitrate group, which is distinguished from the difference of 94 cm^{-1} between the two highest frequencies. For the compound **4**, the strong bands at 1170 cm^{-1} and 1030 cm^{-1} (ν3) and the medium bands at 928 cm^{-1} (ν1) and 646 cm^{-1} (ν4) are attributed to monocoordinated sulfato group [19]. The vanadyl complex shows two intense sharp bands at 945 cm^{-1} and 617 cm^{-1} due to V=O and V-O (enolic) stretching vibrations respectively [20]. From the IR spectra, it is perceived that HL^{5} uses pyridine nitrogen, azomethine nitrogen and ketoamine or enolimine oxygen for coordination, thereby acts as a N, N, O tridentate ligand.

Table 2

Infrared spectral assignments (cm^{-1}) for HL and its complexes

Compound	ν(^{2}NH)	ν(C=N)	ν(C=O)	ν(N=C)	ν(N–N)	ν(M–N)	ν(M–O)
HL	3376	1597	1694	____	1143	____	____
$[Co(L)(NO_3)]\cdot 2H_2O$ (**1**)	____	1564	____	1500	1150	449	505
$[Ni(L)(NO_3)]$ (**2**)	____	1545	____	1489	1145	417	507
$[Cu(L)_2]$ (**3**)	____	1562	____	1540	1146	421	505
$[Zn(HL)(SO_4)(OMe)]\cdot H_2O$ (**4**)	3220	1560	1664	____	1145	472	600
[(VO)(L)(OMe)] (**5**)	____	1568	____	1530	1147	512	612

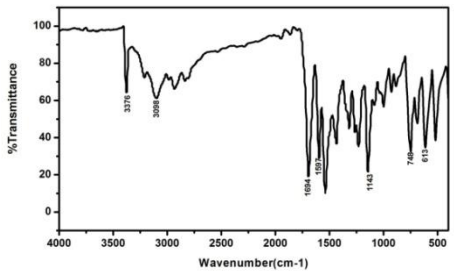

Fig. 1 IR spectrum of HL

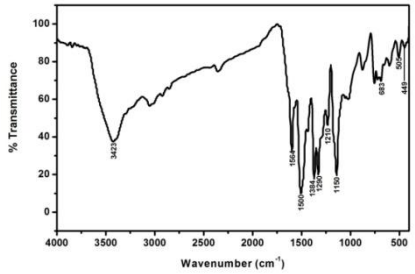

Fig. 2 IR spectrum of $[Co(L)(NO_3)]\cdot 2H_2O$

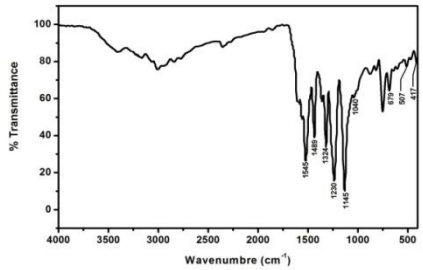

Fig. 3 IR spectrum of $[Ni(L)(NO_3)]$

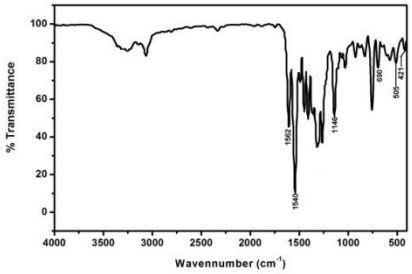

Fig. 4 IR spectrum of $[Cu(L)_2]$

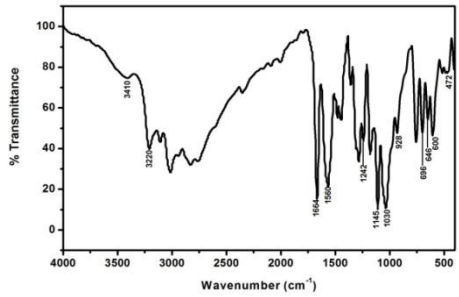

Fig. 5 IR spectrum of $[Zn(HL)(OMe)(SO_4)]\cdot H_2O$

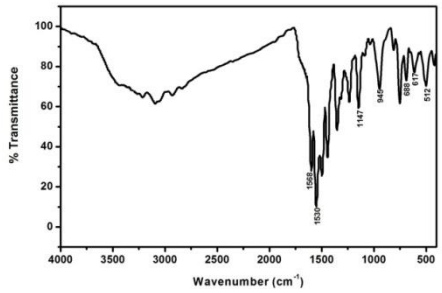

Fig. 6 IR spectrum of [(VO)(L)(OMe)]

3.3 Electronic Spectra

The electronic spectra of HL and its complexes recorded in DMF solution are shown in Figs. 7 to 12 respectively and the spectral assignments are given in Table 3. The bands at 243 nm, 323 nm and 355 nm in the ligand are assigned to the π–π* and n–π* transitions of phenyl rings and semicarbazone moiety respectively. These intraligand bands are subjected to some positive shifts during complexation [21]. The high energy n–π* transition due to the pyridine ring also alters in position, showing pyridine nitrogen coordination. But this peak is not distinguishable in most of the complexes due to the presence of high intensity charge transfer bands. Similarly the charge transfer bands also mask the *d-d* bands and we cannot detect them precisely.

International Journal of Advance Research in Science and Engineering
Volume No 06, Special Issue No. 03, September 2017, AFM-2017
www.ijarse.com
IJARSE
ISSN: 2319-8354

Table 3

Electronic spectral assignments (nm) of HL and its complexes

Compound	d–d	LMCT/ MLCT	n–π*	π–π*
HL	___	___	323, 355	243
$[Co(L)(NO_3)]\cdot 2H_2O$ (**1**)	651	451	374	304
$[Ni(L)(NO_3)]$ (**2**)	560	457	350	270
$[Cu(L)_2]$ (**3**)	738	425	357	268
$[Zn(HL)(SO_4)(OMe)]\cdot H_2O$ (**4**)	___	550	335, 402	258
[(VO)(L)(OMe)] (**5**)	___	435	336, 398	257

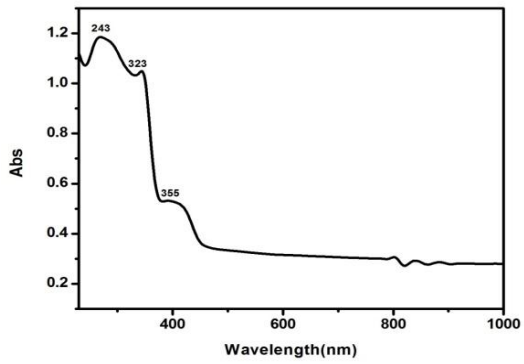

Fig. 7 Electronic spectrum of HL

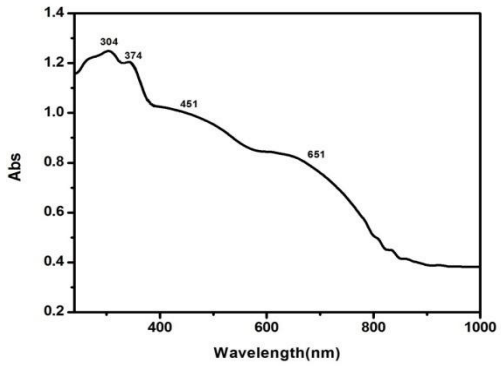

Fig. 8 Electronic spectrum of $[Co(L)(NO_3)]\cdot 2H_2O$

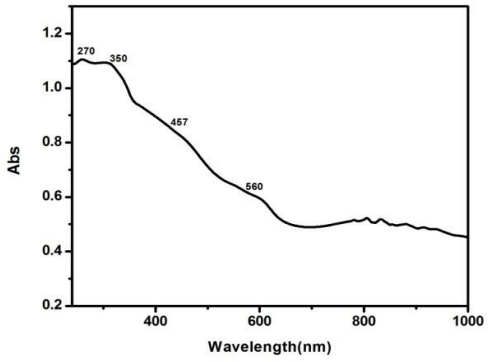

Fig. 9 Electronic spectrum of $[Ni(L)(NO_3)]$

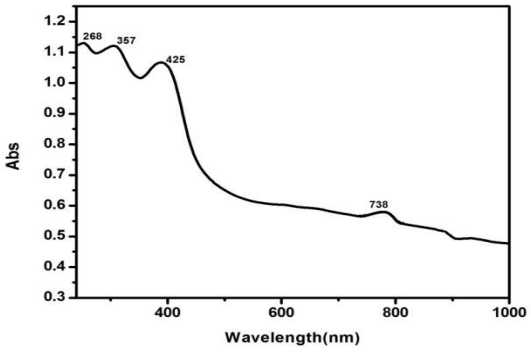

Fig. 10 Electronic spectrum of $[Cu(L)_2]$

International Journal of Advance Research in Science and Engineering
Volume No 06, Special Issue No. 03, September 2017, AFM-2017
www.ijarse.com
IJARSE
ISSN: 2319-8354

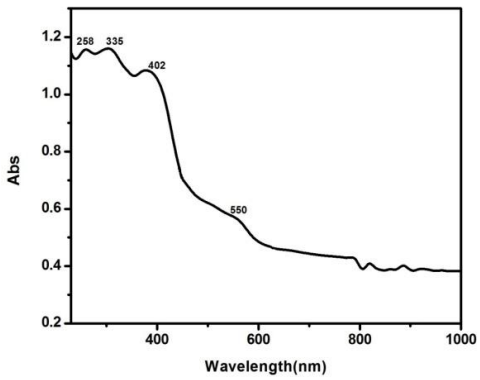

Fig. 11 Electronic spectrum of $[Zn(HL)(OMe)(SO_4)]\cdot H_2O$

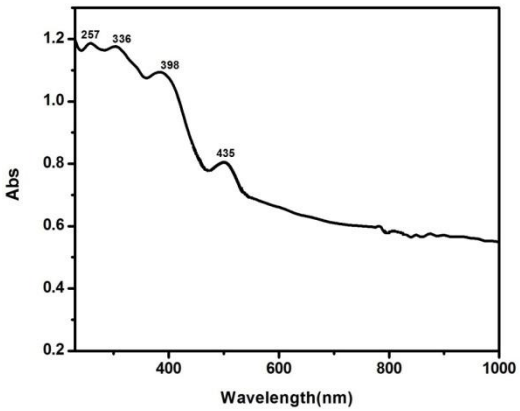

Fig. 12 Electronic spectrum of [(VO)(L)(OMe)]

3.4 Mass Spectra of HL and complexes

The ESI mass spectrum of the ligand and its complexes are disposed in Figs. 12 to 17. The mass spectrum of HL consists of peaks at 120.05588, 148.05071, 170.03262 and 263.09070 due to $[HL-(C_6H_6N_3)]^+$, $[HL-(C_6H_6N)]^+$, $[HL-(C_2H_2N_2O)]^+$ and $[HL+Na]^+$ respectively. The base peak is due to the adduct ion $[(HL)+Na]^+$. The absence of $[M+(HL)_2-2H]^+$ ion in the mass spectrum of cobalt complex excludes the chance of oxidation of the metal. The complexes with $[M+2(HL)–H]^+$ peak as dominant ion exist in 1:2 ratio whereas those with $[M+(HL)–H]^+$ cationic species exist in 1:1 ratio. The base peaks for **1**, **2**, **3**, **4** and **5** are observed at 298.00221, 254.02291, 302.02291, 263.09095 and 263.09108 due to $[M+(HL)-H]^+$, $[(HL)+(NH)-H]^+$, $[M+(HL)-H]^+$, $[(HL)+Na]^+$ and $[(HL)+Na]^+$ [22].

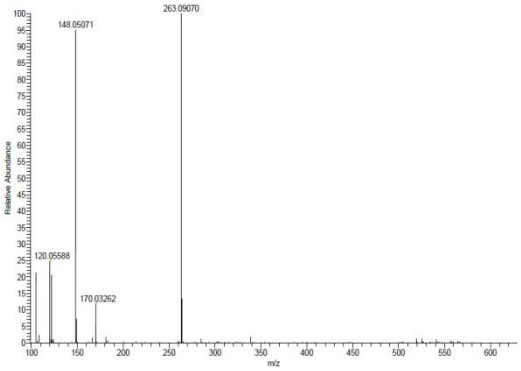

Fig. 12 Mass spectrum of HL

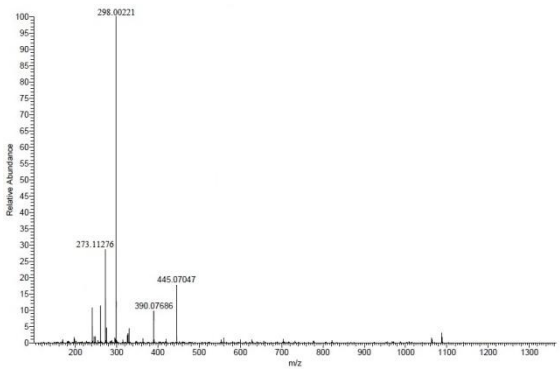

Fig. 13 Mass spectrum of $[Co(L)(NO_3)]\cdot 2H_2O$

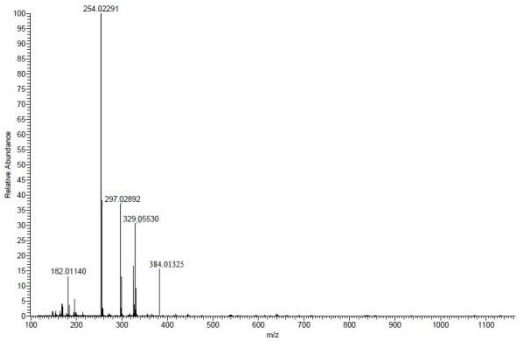

Fig. 14 Mass spectrum of [Ni(L)(NO_3)]

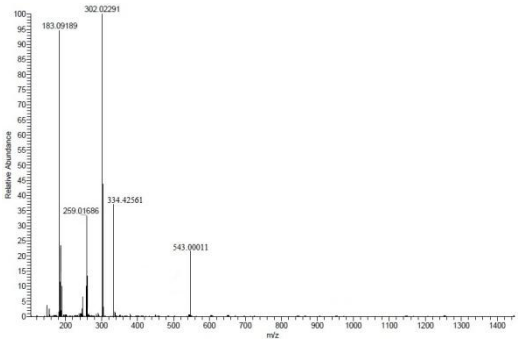

Fig. 15 Mass spectrum of [$Cu(L)_2$]

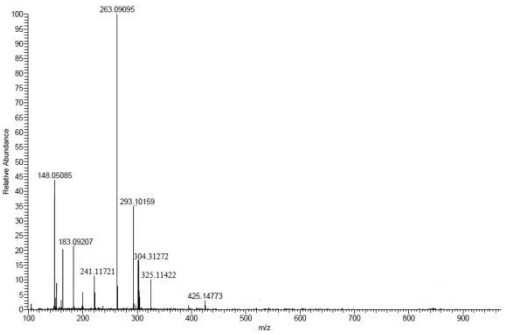

Fig. 16 Mass spectrum of [Zn(HL)(OMe)(SO_4)]·H_2O

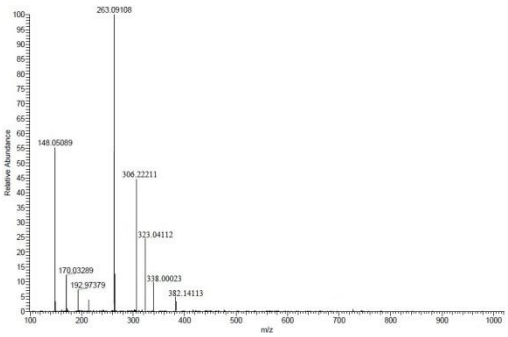

Fig. 17 Mass spectrum of [(VO)(L)(OMe)]

3.5 Biological studies

3.5.1 Amtimicrobial screening

HL and its copper(II) complex were tested for antibacterial activity against four pathogenic bacteria (*Pseudomonas aeroginosa*, *E.coli*, *Staphylococcus aureus*, *Enterococcus faecalis*) and antifungal activity against two fungi (*Candida albicans* and *Aspergillus niger*) using agar well diffusion method. The diameter of zone of inhibition formed around the wells was calculated for three different concentrations (25 µl, 50 µl and 100 µl) using a standard drug. The diameter of zone of inhibition of the compounds is presented in Table 4. HL showed less or zero antibacterial activity at lower concentrations and greater inhibitory effect at higher concentrations. The copper(II) complex showed partial antibacterial activity even at low concentrations and somewhat higher activity than the ligand. At lower concentration the compounds were inactive against *Candida albicans*, whereas showed moderate activity against *Aspergillus niger*. At higher concentrations, both the compounds inhibited strong antimycobial activity.

Table 4

Diameter of zone of inhibition of compounds in cm

Compound	*P.aeruginosa*			*E.coli*			*S. aureus*			*E.faecalis*			*Candida albicans*			*Aspergillus niger*		
	25	50	100	25	50	100	25	50	100	25	50	100	25	50	100	25	50	100
HL	——	1.2	1.9	——	1.1	2.0	——	1.3	1.7	——	1.1	1.9	——	1.1	1.5	1.1	1.3	1.7
$[Cu(L)_2]$	1.0	1.5	2.3	1.0	1.2	1.6	1.1	1.3	1.9	——	1.1	2.0	——	1.0	1.9	1.0	1.2	1.9

3.5.2 Antioxidant Assay

The antioxidant activity of the compounds were investigated using 1,1-diphenyl-2-picrylhydrazyl (DPPH) assay. The standard selected was ascorbic acid. DPPH assay measures the ability of a drug to donate hydrogen [23]. Thus the reducing capability or the antioxidant property of a drug is measured with respect to the change in optical density of DPPH. Concentration of HL and its copper complex and their corresponding percentage of inhibition are given in Table 5. The percentage of inhibition against concentration graph of the compounds is displayed in Fig. 18. DPPH assay suggests that HL and its copper complex have considerable antioxidant properties. Based on the IC_{50} values obtained from the graph, the scavenging ability of the complex is found to be greater than the ligand. Hence they can be used for the preparation of drugs for the treatment of diseases like arteriosclerosis, neurodegenerative and cardiovascular diseases,etc.

Table 5

The percentage of inhibition of the compounds at different concentrations

Concentration(µg/mL)	Percentage of inhibition		
	Standard	HL	$[Cu(L)_2]$
12.5	46.92	21.68	40.30
25	59.75	26.09	48.81
50	73.90	34.43	57.15
100	80.94	43.30	62.55
200	89.08	53.58	72.61

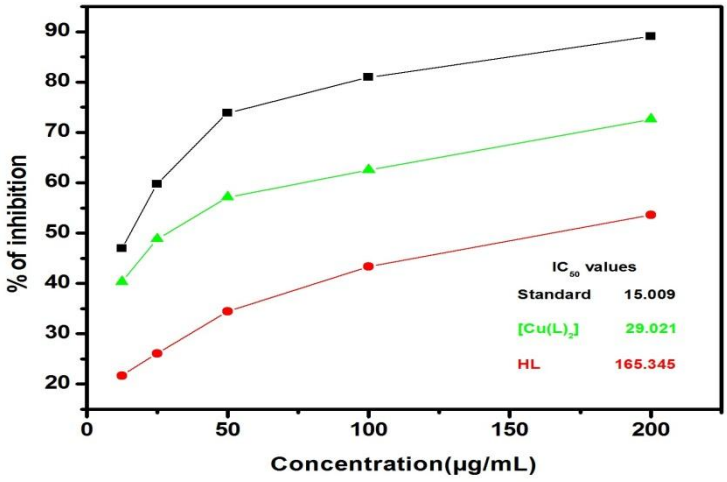

Fig. 18 Concentration vs. % of inhibition graph of compounds

3.5.3 *In vitro* DNA cleavage Assay

DNA cleavage implies breaking of one of the phosphodiester chains of super coiled DNA and produces open circular form and linear form. In the present study we assessed the ability of HL and the copper complex to cleave plasmid pUC18 DNA in presence of the oxidant H_2O_2. The results of DNA cleavage studies have been displayed in

Fig. 19. The control experiment using DNA alone does not show any significant cleavage of the plasmid. The copper complex only cleaves the super coiled pUC18 DNA into linear form. Copper ions react with H_2O_2 and produces hydroxyl ions which then attack the DNA strands [24].

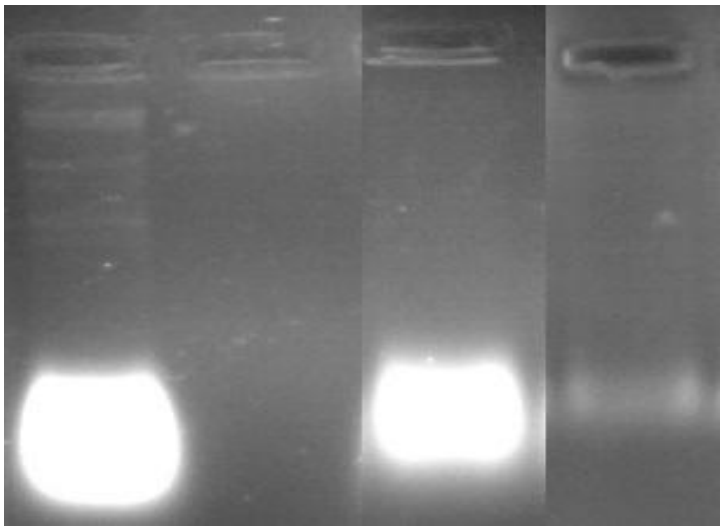

Fig. 19 Cleavage of pUC18 DNA induced by H_2O_2

Lane 1: pUC18 DNA alone, Lane 2: pUC18 DNA+ Fenton's Reagent, Lane 3: pUC18 DNA+ HL, Lane 4: pUC18 DNA+ $Cu(L)_2$

4 CONCLUSION

Pyridine-2-carboxaldehyde-N(4)-phenyl semicarbazone and its complexes were synthesized. The molecular formulae of the complexes were determined by elemental analyses and conductivity studies. The room temperature magnetic susceptibility studies reveal the oxidation states and the magnetic behavior of the complexes. The neutral or anionic N, N, O tridentate behaviour of the ligand in the complexes were confirmed by FT-IR, UV-Visible, NMR and mass spectral technique. The copper complex showed greater antimicrobial and antioxidant actvities compared to the semicarbazone owing to greater lipophilicity. The *in vitro* DNA cleaving assay showed higher activity for the copper complex.

5 ACKNOWLEDGMENTS

The authors are grateful to SAIF, Cochin University of Science and Technology for elemental analysis, FT–IR and UV–visible spectral analysis, SAIF, IIT Chennai for room temperature magnetic susceptibility measurement, NIIST, Thiruvananthapuram, for mass spectral analyses. One of the authors, LSR gratefully acknowledges CSIR, New Delhi for the award of Senior Research Fellowship.

6 REFERENCES

[1] V. L. Siji, M. R. Sudarsanakumar, S. Suma, M. R. P. Kurup, Spectrochim. Acta, 76 A(1), 22, 2010.

[2] T. A. Reena, E. B. Seena, M. R. P. Kurup, Polyhedron, 27**,** 1825, 2008.

[3] H. Beraldo, D. Gambino, Mini Rev. Med. Chem., 4(1), 31, 2004.

[4] M. J. Ahsan, Cent. Nerv. Syst. Agents Med. Chem., 13, 148, 2013.

[5] V. Mishra, S. N. Pandeya, C. Pannecouque, M. Witvrouw, E. De Clercq, Arch. Pharm. Pharm. Med. Chem., 5, 183, 2002.

[6] Z. Afrasiabi, R. Almudhafar, D. Xiao, E. Sinn, A. Choudhury, A. Ahmad, A. Vyas, F. Sarkar, S. Padhye, Trans. Met. Chem., 38(6), 665, 2013.

[7] R. L.; Shriner, R. C. Fuson, The Systematic Identification of Organic Compounds, 3rd ed., John Wiley & Sons. Inc., 1980.

[8] N. M. R. Jamal, J. Mokhtari, M. G. Dekamin, S. Javanshir, Iran. J. Chem. Chem. Eng., 31(2), 1, 2012.

[9] Yu. M. Chumakov, V. I. Tsapkov, B. Ya. Antosyak, N. N. Bairac, Yu. A. Simonov, G. Bocelli, E. Pahontu, A. P. Gulea, Crystallography Reports, 54(3), 455, 2009.

[10] M. S. Refat, S. Chandra, M. Tyagi, Therm. Anal. Calorim., 100**,** 261, 2009.

[11] J. Wiecek, D. Kovala-Demertzi, Z. Ciunik, J. Wietrzyk, M. Zervou, M. Demertzis, Bioinorg. Chem. Appl., 2010.

[12] L. Lin, W. Fan, S. Chen, J. Ma, W. Hu, Y. Lin, H. Zhang, R. Huang, New J. Chem., **36**, 2562, 2012.

[13] H. W. Chang, D. A. Julin, J. Biol. Chem., 276, 46004, 2001.

[14] W. J. Geary, Coord. Chem. Rev., **7**, 81, 1971.

[15] J. R. Anacona, G. Da Silva, 50**,** 447, 2005.

[16] A. A. A. Abu-Hussen, A. A. A. Emara, J. Coord. Chem., 57(11), 973, 2004.

[17] D. X. West, J. K. Swearingen, Transit. Met. Chem., 26, 260, 2001.

[18] S. Chandra, L. K. Gupta, Spectrochim. Acta, A 62, 1089, 2005.

[19] K. Nakamoto, Infrared and Raman Spectra of Inorganic and Coordination Compounds, 4th ed., Wiley, New York, 1986.

[20] E. Manoj, M. R. P. Kurup, Polyhedron, 27(1), 275, 2008.

[21] S. Goel, S. Chandra, S. D. Dwivedi, J. Saudi Chem. Soc., 20, 651, 2016.

[22] P. E. Aranha, M. P. dos Santos, S. Romera, E. R. Dockal, Polyhedron, 26(7), 1373, 2007.

[23] I. P. Ejidike, P. A. Ajibade, J. Coord. Chem., 68(14), 2552, 2015.

[24] D. Tilala, H. Gohel, V, Dhinoja, D. Karia, Int. J. Chemtech Res., 5(5), 2329, 2013.